

## Thermal-pressure loading effect on containment structure

Hyo-Gyoung Kwak\* and Yangsu Kwon<sup>a</sup>

Department of Civil Engineering, Korean Advanced Institute for Science and Technology,  
291 Daehak-ro, Yuseong-gu, Daejeon 305-701, Republic of Korea

(Received December 6, 2013, Revised March 4, 2014, Accepted March 19, 2014)

**Abstract.** Because the elevated temperature degrades the mechanical properties of materials used in containments, the global behavior of containments subjected to the internal pressure under high temperature is remarkably different from that subjected to the internal pressure only. This paper concentrates on the nonlinear finite element analyses of the nuclear power plant containment structures, and the importance for the consideration of the elevated temperature effect has been emphasized because severe accident usually accompanies internal high pressure together with a high temperature increase. In addition to the consideration of nonlinear effects in the containment structure such as the tension stiffening and bond-slip effects, the change in material properties under elevated temperature is also taken into account. This paper, accordingly, focuses on the three-dimensional nonlinear analyses with thermal effects. Upon the comparison of experiment data with numerical results for the SNL 1/4 PCCV tested by internal pressure only, three-dimensional analyses for the same structure have been performed by considering internal pressure and temperature loadings designed for two kinds of severe accidents of Saturated Station Condition (SSC) and Station Black-out Scenario (SBO). Through the difference in the structural behavior of containment structures according to the addition of temperature loading, the importance of elevated temperature effect on the ultimate resisting capacity of PCCV has been emphasized.

**Keywords:** 1/4 PCCV; PSC structure; un-bonded tendon; nonlinear behavior; thermal loading

---

### 1. Introduction

One of the major structures in a nuclear power plant (NPP) is a massive containment structure which surrounds the nuclear power furnace and related components. Such a containment structure has a thick walled prestressed concrete (PSC) cylindrical shell with a hemispherical dome, whose design has been strictly guided by related design codes (NRC), and an exact prediction of its ultimate resisting capacity under extreme design loads is also essential in design procedure because it serves as a final barrier to prevent the dissemination of radioactive materials in any case of accident.

A lot of experimental studies (Rizkalla *et al.* 1984, Twidale and Crowder 1991, Hessheimer *et al.* 2003, Kevrokian *et al.* 2005, Parmar *et al.* 2013) have been concentrated on internal pressurization tests to check if newly designed containment structures still maintain the resisting

---

\*Corresponding author, Professor, E-mail: khg@kaist.ac.kr

<sup>a</sup>Ph.D. Student, E-mail: ifyou169@gmail.com

capacity while representing the expected failure behavior even in the case of pressure loading beyond the design basis accident. Moreover, the obtained experimental results have also been used as the reference values for the numerical analyses to improve the accuracy in numerical results depending on the modeling of structure. Among scale model experiments of containment structures, a 1/14 scale model of Gentilly-2 in Canada (Rizkalla *et al.* 1984), a 1/10 scale model of Sizewell-B in UK (Twidale and Crowder 1991), a 1/4 scale model of Ohi-3 in the US (Hessheimer *et al.* 2003), and MAEVA mock-up in France (Kevrokian *et al.* 2005) can be considered as representative experimental studies. In addition, many numerical analyses for containment structures (Yonezawa *et al.* 2002, Dameron *et al.* 2003, Hessheimer and Dameron 2006, Hu and Lin 2006, Lee 2011) have also been concentrated on the pressure loading condition.

On the other hand, the change in temperature at the concrete containment structures has no attention in the analyses and design practice even though a core failure at the interior of structure accompanies far beyond operating temperature together with high pressure. It seems to be induced from the assumption that the containment structure made of concrete with the relatively low thermal conductivity will not be exposed to high temperature for a long time even in the case of severe accident in a NPP. No experimental study has also been conducted to evaluate the safety of containment structures subjected to internal pressure with high temperature due to the difficulties in experiment. In addition, very limited numbers of simplified numerical analyses have been introduced with the objective of predicting the temperature loading effect (Hessheimer and dameron 2006, Nahas and Cirée 2009, Davie and Pearce 2014) and blast load cases (Dong *et al.* 2010). Temperature time history proposed at Phase 3 of ISP-48 (2005) has been considered as the reference temperature history used in the analysis and design practice.

However, since elevated temperature causes not only the development of additional thermal loadings but also the change in material properties of concrete and steel, an exact evaluation for the nonlinear behavior of containment structures faced to high temperature in the cases of a severe accident must be based on the implementation of material properties depending on the temperature change (Bazant and Kaplan 1996, Kodur *et al.* 2010). A review of the mechanical properties of concrete at elevated temperature is given by Phan and Carino (1998). Effects of elevated temperatures include decreasing the compressive strength of concrete and increasing the absolute strain value corresponding to it, and many stress-strain relationships as well as the creep deformation for concrete at elevated temperature have been proposed on the basis of experimental data (Anderberg and Thelandersson 1976). The change in the mechanical properties of steel at elevated temperature is not exceptional. An increasing of strain and a decrease of strength with high temperature has been reflected in many stress-strain relationships of steel (Kodur *et al.* 2010).

This paper, accordingly, concentrates on the three-dimensional analyses of containment structures subjected to elevated temperature as well as internal pressure. Different from the previous numerical analyses that ignored the temperature effect and/or the three-dimensional effect induced from many holes in the wall of containment structure, a more rigorous nonlinear three-dimensional analyses haven been performed by considering internal pressure and temperature loadings and the change in mechanical properties of concrete and steel under high temperature has been implemented, to extend the understating of capacities of actual containment structures. Upon the numerical results for the containment structures under pressure loading only, the difference in the structural behavior of containment structures according to the addition of temperature loading has been reviewed. Furthermore, the importance of high temperature effect on the ultimate resisting capacity of PCCV has been emphasized.

## 2. Material models

### 2.1 Concrete material model

As a PSC containment structure is one of the cylinder-type structures and carries out-of-plane loadings, the biaxial stress condition must also be taken into account to simulate the exact structural behavior according to the loading history. Under combinations of the biaxial stress, however, the stress–strain behavior of concrete is different from those under uniaxial loading conditions owing to the effects of Poisson's ratio and micro-crack confinement. To simulate the stress state of concrete under biaxial loading, the orthotropic model is adopted in this paper for its simplicity and computational efficiency. With reference to the principal axes of orthotropic, the incremental constitutive relationship can be expressed by

$$\begin{Bmatrix} d\sigma_1 \\ d\sigma_2 \\ d\sigma_3 \end{Bmatrix} = \frac{1}{1-\nu^2} \begin{bmatrix} E_1 & \nu\sqrt{E_1E_2} & 0 \\ \nu\sqrt{E_1E_2} & E_2 & 0 \\ 0 & 0 & (1-\nu^2)G \end{bmatrix} \begin{Bmatrix} d\varepsilon_1 \\ d\varepsilon_2 \\ d\varepsilon_3 \end{Bmatrix} \quad (1)$$

where  $(1-\nu^2)G = 0.25[E_1 + E_2 - 2\nu(E_1E_2)^{\frac{1}{2}}]$ ,  $E_1$  and  $E_2$  are the secant moduli of the elasticity in the direction of the axes of orthotropic, which are oriented perpendicular and parallel to the crack direction. Additionally,  $G$  is the shear modulus of the elasticity and  $\nu$  is Poisson's ratio.

The use of the orthotropic constitutive relationship in Eq. (1) to represent a cracked concrete may not be entirely realistic. In the case of a real crack, the crack surface is rough and any sliding parallel to the crack will generate some local stresses or movements normal to the crack. To represent this type of nonlinear behavior properly, the off-diagonal terms of the material matrix that relate the shear strain with the normal stress should not be zero. The relative magnitude of these off-diagonal terms decreases as the crack widens. This effect may not, however, be significant in a study that focuses attention on the overall structural behavior, and most researchers have neglected it (Kwak and Kim 2004a, b).

The proposed concrete model accounts for progressive cracking and changes in the crack direction by assuming that the crack is always normal to the total principal strain direction (the rotation crack model). More details can be found in work by Kwak and Kim (2006a). When the principal tensile strain exceeds the ultimate tensile strain  $\varepsilon_{cu,T}$ , the material only loses its tensile strength normal to the crack while it is assumed to retain its strength parallel to the crack direction.

Total uniaxial strain of concrete  $\varepsilon_{tot,c}(t)$  at time  $t$  after severe accident can be divided into two parts of mechanical strain  $\varepsilon_{m,c}(t)$  and non-mechanical strain  $\varepsilon_{nm,c}(t)$ , and the non-mechanical strain has been composed of thermal strain  $\varepsilon_{th}$ , creep strain  $\varepsilon_{cr}$  and transient strain  $\varepsilon_{tr}$  in the case of concrete subjected to high temperature.

$$\Delta\varepsilon_{tot,c}(t) = \Delta\varepsilon_{m,c}(t) + \Delta\varepsilon_{nm,c}(t) = \Delta\varepsilon_{m,c}(\sigma, T) + \Delta\varepsilon_{th,c}(T) + \Delta\varepsilon_{cr,c}(\sigma, T, t) + \Delta\varepsilon_{tr,c}(\sigma, T) \quad (2)$$

where  $\sigma$  means the stress of concrete at temperature  $T$ . Thermal strain  $\varepsilon_{th,c}(T)$  is induced from expansion of the concrete medium by elevated temperature and corresponding equations to take into account the thermal expansion of concrete can be found elsewhere (Lie and Chabot 1990, Eurocode 2 2004). Among those equations, related equations proposed in Eurocode 2 (2004) have been used in this paper for the evaluation of thermal strain component because these equations

have effectively considered non-linearity by the temperature change as well as by the physical and chemical changes of concrete medium at the high temperature. Different from thermal strain, however, the creep deformation of concrete has not clearly been verified, and still many related experiments have been performed with the suggestion of relations (Anderberg 1988, Schneider 1988). Among those models, a creep model proposed by Harmathy (1993) is adopted in this paper because it can effectively consider the stress condition of concrete, fire duration time and temperature increase by the fire.

$$\Delta\varepsilon_{cr,c} = \beta_1 \frac{\sigma}{f'_{cT}} \cdot \sqrt{t} \cdot e^{k_1(T-293)} \quad (3)$$

where  $f'_{cT}$  and  $\sigma$  mean the compressive strength and the stress of concrete at temperature  $T$  respectively,  $T(K)$  is concrete temperature (kelvin), and  $t$  is fire elapsed time (second). And, constants  $\beta_1=6.28 \times 10^{-6} \text{sec}^{-0.5}$  and  $k_1=2.658 \times 10^{-3} K^{-1}$  determined from experiment by Cruz (1968) are used. In addition to thermal and creep strains, additional creep strain has been induced in the concrete medium by the physical and chemical changes in material composition and it is called as transient strain  $\varepsilon_{tr}$ . To take into account this non-mechanical deformation, a model introduced by Anderberg and Thelandersson (1976) is adopted in this paper because it effectively predicts the progress of transient strain determined from experiment and has the simple form to be implemented into the numerical formulation (see Eq. (4)).

$$\Delta\varepsilon_{tr,c} = -k_2 \frac{\sigma}{f'_c} \varepsilon_{th,c} \quad (4)$$

where  $f'_c$  is the compressive strength of concrete at the room temperature and  $k_2$  is a dimensionless constant of which range is 1.8~2.35. This paper adopts the value of 2.35 which was found at the previous experiment.

On the other hand, concrete stress can be determined by substituting only the mechanical strain component into stress-strain relationship. In describing the uniaxial stress-strain behavior of concrete, many empirical formulas have been proposed, and the consideration of the effect by elevated temperature is not exceptional (Lie and Lin 1985, Anderberg and Thelandersson 1976). In this paper, the stress-strain relationship proposed by Lie and Lin (1985) is used because it is effectively describing the thermal characteristics of concrete ascertained by experiment. Fig. 1 shows the variation of stress-strain relations of concrete according to an increase of temperature.

Upon the determination of the compressive and tensile strength of concrete corresponding to the elevated temperature, accordingly, the biaxial strength envelope must be defined. Fig. 2 shows the adopted biaxial strength envelope of concrete under proportional loading. This strength envelope was proposed by Lee and Fenves (1998) and has been defined in ABAQUS (Dassault Systems 2011). As shown in this figure, the envelope to define the compression-compression region is slightly different from the Kuper's failure envelope (Kupfer and Gerstle 1973) obtained through panel test. The difference, however, will not have different effect in the structural behavior because the nonlinear behavior of a containment structure subjected to internal pressure and temperature loadings are induced from the cracking of concrete by the biaxial stresses placed on the tension-tension region and partially on the compression-tension region. Additional details regarding the envelope curve in tension-tension region can be found in previous study by Kwak and Kim (2004a, 2004b).

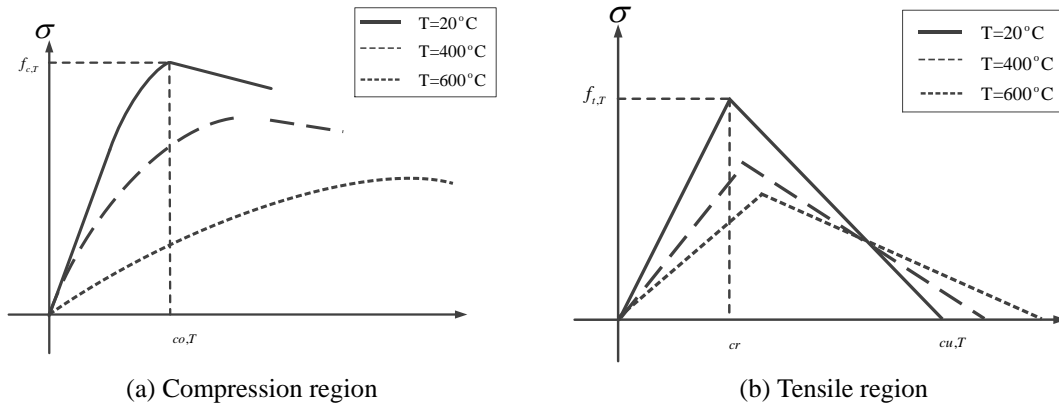


Fig. 1 Stress-strain relation of concrete by elevated temperature

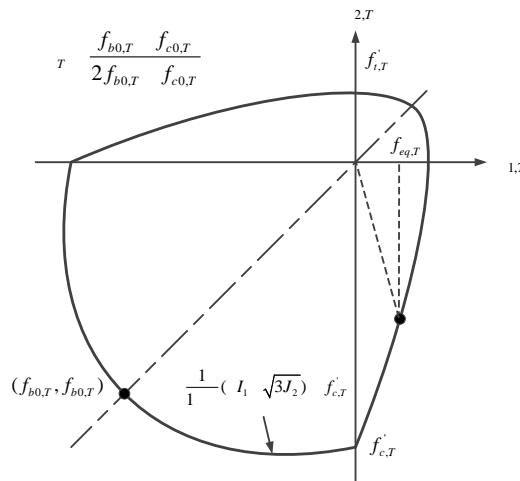


Fig. 2 Biaxial concrete strength envelope (Lee and Fenves 1998)

### 2.2 Steel material model

For modeling the behavior of steel, the stress-strain relation should be defined. Since both mechanical properties of the Young's modulus and the yield strength are degraded with high temperature, the definition of the stress-strain relation of steel according to the elevated temperature is necessary to reflect the degradation of the material properties and many related experimental and analytical research have been performed (Lie and Chabot 1990, Schaffer 1992, Eurocode 2 2004). Among those models, the stress-strain relationship of the steel reinforcement in EN1992-1-2 is used in this paper because a material model. This material model is consisted of 4 different ranges as shown in Fig. 3, and more details related to the definition of each region can be found elsewhere (Eurocode 2 2004). In Fig. 3,  $\sigma_{sp,T}$  and  $\sigma_{sy,T}$  mean the proportional limit and the yield limit and  $\epsilon_{sp,T}$  and  $\epsilon_{sy,T}$  represent the corresponding strains, respectively. The other two limiting strains have the values of  $\epsilon_{st,T}=0.15$  and  $\epsilon_{su,T}=0.2$ .

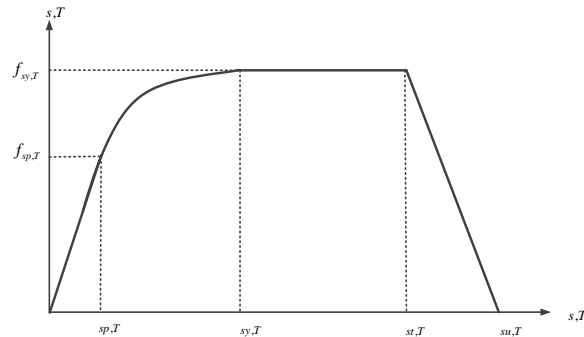
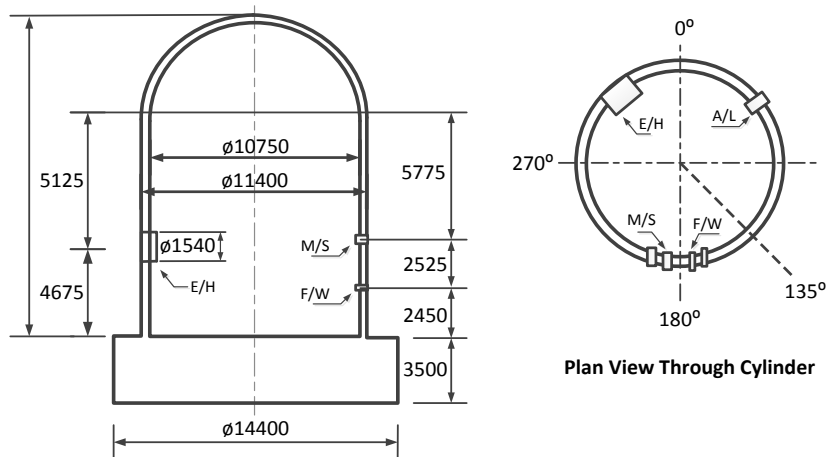


Fig. 3 Stress-strain curve of steel

Fig. 4 Configuration of 1/4 scale PCCV (Hessheimer *et al.* 2003)

### 3. Application

#### 3.1 PWR Containment (1/4 PCCV)

As shown in Fig. 4 which represents the overall geometry of a 1/4 PCCV tested by Sandia National Lab. (Hessheimer *et al.* 2003), the containment is composed of a circular base slab, an upright cylinder with two buttresses to accommodate the anchorages for the prestressing tendons being located symmetrically around the wall and a hemispherical dome. The overall height is 16.4 m, and the radius of the cylinder is 5.3 m. The cylinder's wall thickness is 0.32 m, reducing to 0.275 m in the dome after a short transition region. The bottom of the cylinder is joined to a base that is 3.5 m thick. The concrete has passive reinforcement as well as prestressing tendons in the hoop and longitudinal directions. The passive reinforcement is of mild steel, whereas the prestressing tendon use high-strength steel. The interior of the PCCV is lined with mild steel plate with 1.6 mm thick. The design pressure for the example structure is 0.39 MPa, and details of the geometry and dimensions of the containment are provided in reference (Hessheimer *et al.* 2003, Dameron *et al.* 2003).

Equipment hatches and penetrations on the containment are considered for more exact evaluation of structural behavior induced from non-symmetric configuration of structure (Noh *et al.* 2008). 84,658 three-dimensional solid elements (named C3D10R in ABAQUS) are based in the numerical modeling of the containment from the dome to the foundation, and the passive reinforcements embedded in concrete matrix are considered by using the layered steel model. And, the liner plate is considered by the membrane element (named M3D4R in ABAQUS) and 9000 elements are used. On the other hand, the internal tendons are described by the truss element (named T3D2 in ABAQUS) maintaining the placing space and Fig. 6 shows the 3D finite element idealization of 1/4 PCCV. The material properties of concrete, reinforcing steel and tendon are given in also Table 1, and other assumed material properties not mention are determined on the basis of the CEP-Fib MC90 (1990).

To describe the tensioning sequence in the tendon, sequential loading steps of self-weight, post-tensioning and internal pressure are considered, and the prestressing losses caused by the friction and anchorage slip are taken into account on the basis of the values measured from the Sandia National Laboratories 1:4 scale PCCV experiment (Hessheimer *et al.* 2003). Moreover, Fig. 5 shows the average stress-strain relations of prestressing tendon modified by considering the tension stiffening and bond-slip effects according to the numerical algorithm introduced in this paper. Especially the relation corresponding to the un-bonded internal tendon is constructed through the iteration procedure adopted to take into account the slip effect along the length. In Fig. 5, it can be found that there is a slight difference in the average stress-strain relations between hoop tendon and meridional tendon, and larger slip effect can be expected at the meridional tendon. More details related to the iteration procedure for the un-bonded internal tendons can be found elsewhere (Kwak and Kim 2006b).

Table 1 Material properties used in 1/4 PCCV

Structure	Concrete	Rebar	Liner	Tendon
1/4 PCCV	$E_c = 25700\text{MPa}$	$E_s = 190\text{GPa}$	$E_{liner} = 190\text{GPa}$	<b>seven-wire strand</b>
	$f'_c = 53.4\text{MPa}$	$f_y = 480\text{MPa}$	$f_{liner,y} = 380\text{MPa}$	( $A_p = 339\text{mm}^2$ )
	$f_{cr} = 2.21\text{MPa}$	$f_u = 620\text{MPa}$	$f_{liner,u} = 480\text{MPa}$	$f_{pu} = 1900\text{MPa}$

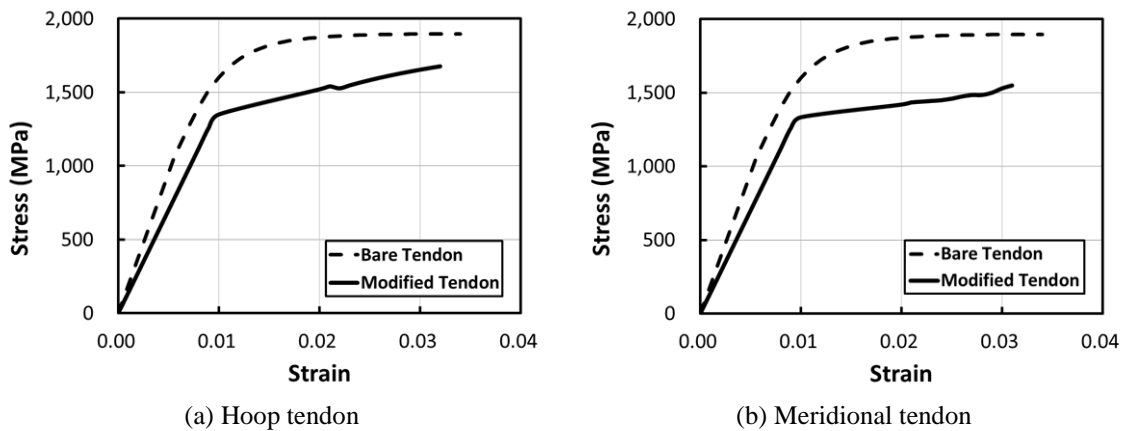


Fig. 5 Modified stress-strain relationships of prestressing tendon

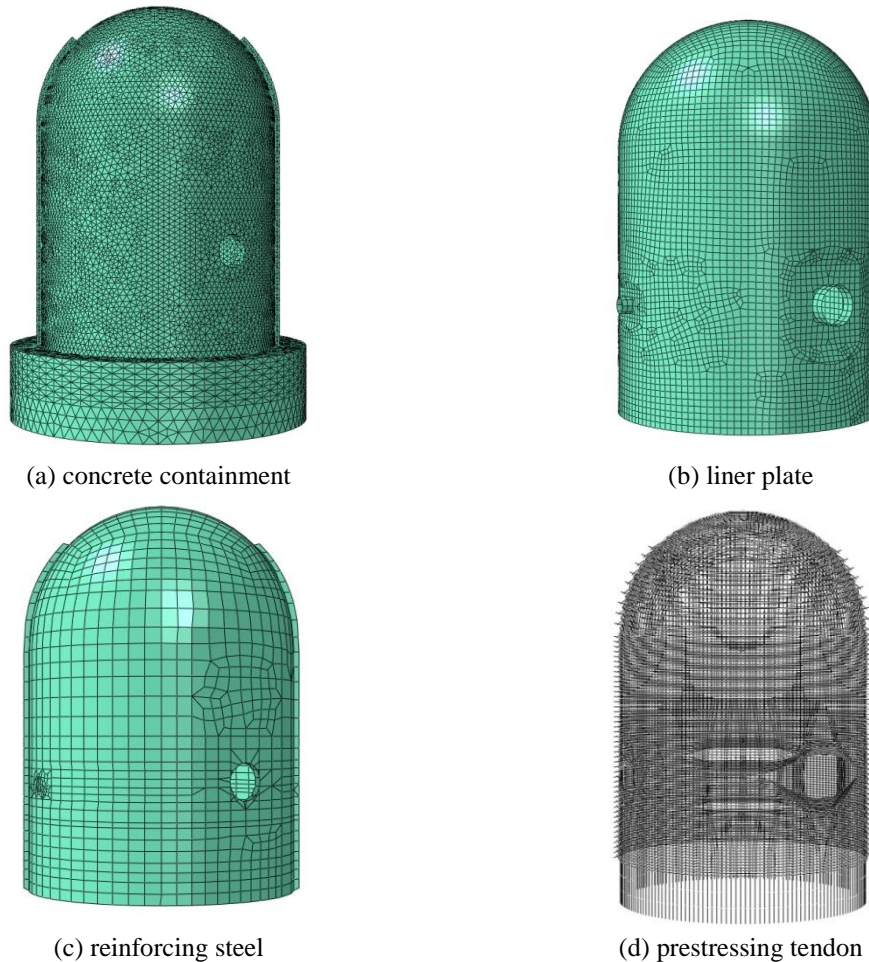
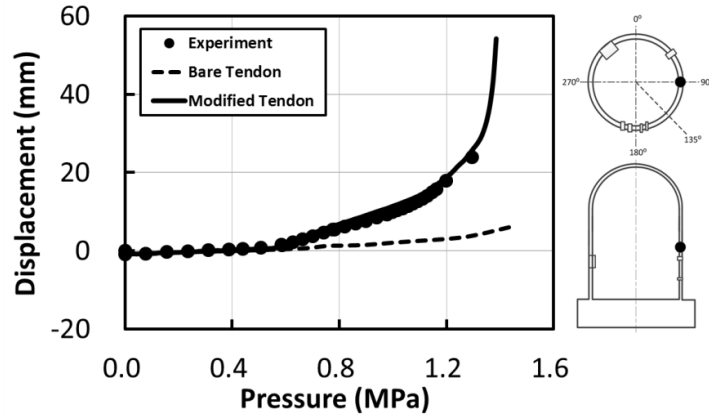
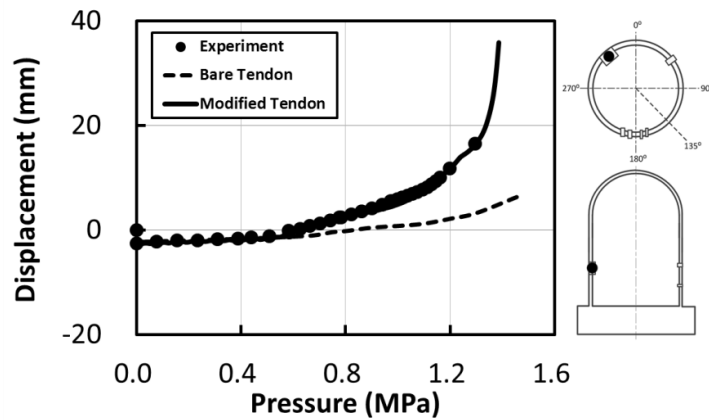


Fig. 6 FE idealization of 1/4 PCCV

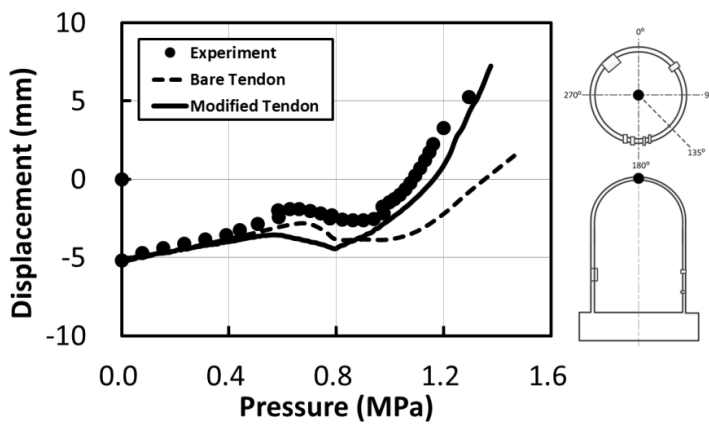
The analytical results obtained by considering all the nonlinear effects are compared with the experimental measurements. To verify the nonlinear effect of tendon, two difference analyses are performed for the same structure, and the obtained results are compared in Fig. 7. Good agreements between analysis results in Modified Tendon and experiment are observed for the entire structural response up to reach the failure stage. Different from Modified Tendon case which considers the nonlinear effects related to the tension stiffening, bond-slip and un-bonded internal tendon, the other result of bare tendon, obtained on the basis of the perfect bond assumption without considering the tension stiffening effect, give more stiff structural responses and larger over-estimation for the ultimate load capacity, and these are corresponding to the generally expected results when the numerical analyses are conducted with commercialized programs. From Fig. 7, it can be found that (1) the most dominant influencing factor on the structural response is the reduction for the yield strength of prestressing tendon when the tension stiffening effect is taken into account through the definition of the strain softening branch in the tensile stress-strain relation of concrete.; (2) the slip behavior along the tendon, accompanied in the case of un-bonded



(a) Mid-height of cylindrical wall



(b) Mid-height of cylindrical wall penetration



(c) Dome apex

Fig. 7 Pressure - Displacement relation of 1/4 PCCV

internal tendon, must be considered to prevent an over-estimation of the ultimate resisting capacity ; and (3) for the reliable prediction of the nonlinear structural response in the containment structure

with un-bonded internal tendons, at least two nonlinear effects of the reduction of yield strength in tendon and the slippage along the tendon must be considered.

### 3.2 PWR Containment under thermal loading

Because of the importance for the consideration of elevated temperature as well as the internal pressure, the OECD-NEA Committee in the Safety of Nuclear Installations (CSNI) suggested a pseudo-pressure/temperature time history (ISP-48 2005) and initiated an International Standard Problem on Containment integrity (ISP-48) based on the NRC/NUPEC/Sandia test with the objective of an exact prediction for the capacities of actual containment structures under a more realistic severe accident. While the previous NPP scale tests and corresponding numerical analyses (Donten *et al.* 1980, MacGregor *et al.* 1980, Hessheimer 2003) were conducted to investigate the response of nuclear containment structures under pressure loading beyond the design basis accident and to compare analytical prediction with measured behavior, ISP-48 was designed to predict the structural response of containment structures to static and transient pressure together with thermal loading.

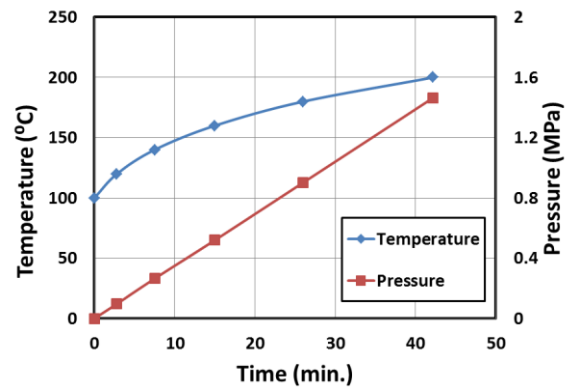
The analytical simulation forms the basis of ISP-48, and two different thermal loading cases are suggested for the application. The first one is for the saturated steam condition which describes the monotonically increasing static pressure and temperatures by saturated steam, and the other one is for the station blackout scenario which represents a severe-accident scenario inducing vessel failure and hydrogen detonation. Time histories of internal pressure and thermal loading for both cases are shown in Fig. 8, pseudo-pressure/temperature time histories were assumed for purposes of the response calculation (ISP-48 2005). Especially the peak pressure and temperature at  $t=250$  min. in Fig. 8(b) were designed to describe a hydrogen burn/detonation. More details related to the description of each loading cases can be found elsewhere (ISP-48 2005, Hessheimer and dameron 2006).

Before application of thermal loading to the same structure of a 1/4 PCCV 3D-model, the heat transfer analysis was conducted to evaluate the distribution of temperature across the section and to determine the corresponding material properties of concrete and steel depending on the changed temperature. Since the thermal response does not scale geometrically, a full scale version of the same PCCV was used in the heat transfer analysis. Then, the resulting temperature gradients are re-scaled and applied to the 1/4 PCCV model for combined thermal-pressure analysis.

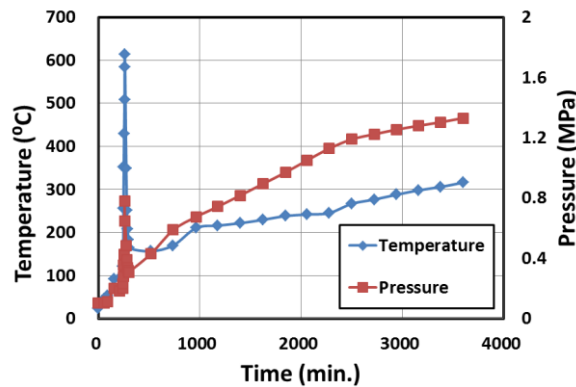
A commercialized program of ABAQUS was used in the heat transfer analysis, and the finite element with temperature degrees of freedom only (Dassault Systems 2011) was used. The base material properties of containment were obtained from the reports of NUREG-6809 (Dameron *et al.* 2003) and NUREG-6810 (Hessheimer *et al.* 2003) which describes the material properties of 1/4 PCCV used in the experiment. Thermal bonding conditions were imposed at the outer surface of the PCCV cylinder and dome wall consisting of free convection with air of a temperature 25°C. The only difference from the previous research is the use of 3D model instead of axisymmetric model. Fig. 9 shows the temperature distribution across a typical section in the wall. As shown in these figures, both analytical results of considering and ignoring the change in material properties with temperature do not represent the remarkable difference for both temperature time histories. It means that the change in material properties with temperature does not affect to the temperature distribution itself and has a minor effect on the evaluation of temperature loading to apply to the containment structures.

Under the same numerical modeling of containment structures with that used in the case of the

pressure loading only, time histories of internal pressure and thermal loading in Fig. 8 are applied and the obtained results can be found in Figs. 10 and 11. In comparison with those obtained by ignoring the thermal loading, similar reductions of more than 20% in the ultimate resisting capacity of the containment structure were occurred for both different temperature time histories. Moreover, it can be found that, different from the distribution of temperature loading in Fig. 8, the structural responses is affected by the change in the material properties at the elevated temperature. Both analyses of considering (w/ degradation in Figs. 10 and 11) and ignoring (w/o degradation in Figs. 10 and 11) the change in the material properties at the elevated temperature were conducted while applying the temperature loading simultaneously with pressure loading, and the following results were also obtained: (1) more remarkable difference in the ultimate resisting capacities between considering and ignoring the change in the material properties with temperature was occurred at Case 1 loading history in Fig. 8; (2) Case 2 loading history developed larger deformations through the whole structure because of relatively higher maximum temperature which accompanies not only an increase of the temperature loading but also a larger decrease of the structural stiffness across the depth of wall and dome; but (3) the additional consideration of the temperature loading changes neither the failure mode nor the critical location where the structural failure starts (see Table 2).



(a) Case 1 Saturated station condition

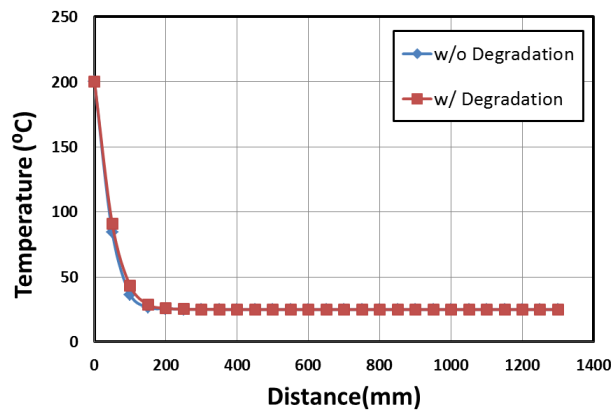


(b) Case 2 Station blackout scenario

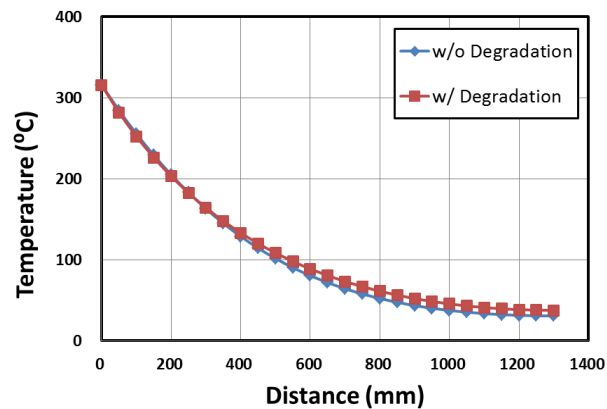
Fig. 8 Pseudo-pressure/temperature time histories (ISP-48 2005)

Table 2 Ultimate pressure (load) and failure mechanism

Case	Crack Occurring (MPa)	Yield of Liner Plate (MPa)	Ultimate Pressure (MPa)	Failure Mechanism
Experiment	0.59~0.78	1.1	1.294	Yield of Liner Plate
Only Pressure (See Fig. 6)	0.56	1.25	1.386	Yield of Liner Plate
Case 1 : w/o degradation (See Fig. 10)	0.55	1.15	1.365	Yield of Liner Plate
Case 1 : w/ degradation (See Fig. 10)	0.51	1.08	1.227	Yield of Liner Plate
Case 2 : w/o degradation (See Fig. 11)	0.55	1.1	1.2635	Yield of Liner Plate
Case 2 : w/ degradation (See Fig. 11)	0.50	0.65	1.2006	Yield of Liner Plate

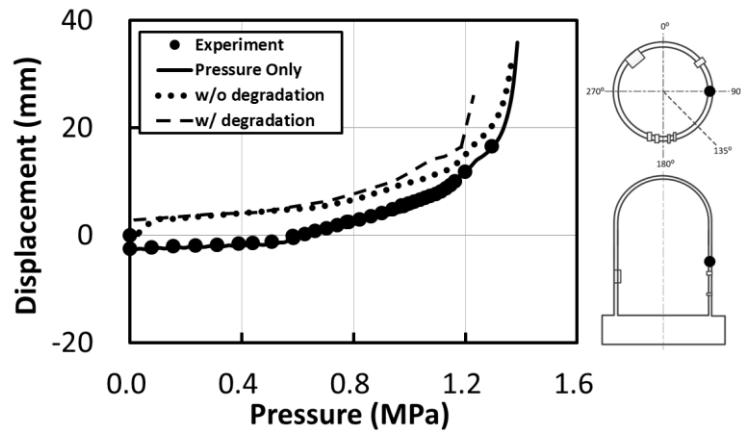


(a) Temperature distribution for Case 1 loading

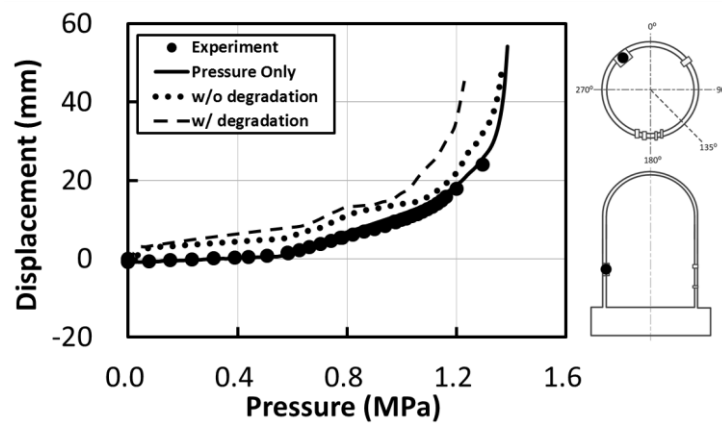


(b) Temperature distribution for Case 2 loading

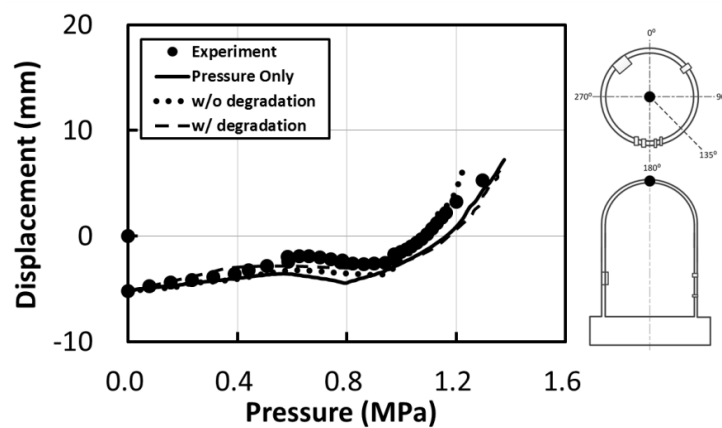
Fig. 9 Temperature distribution across the wall under the maximum temperature



(a) Mid-height of cylindrical wall



(b) Mid-height of cylindrical (wall penetration)



(c) Dome apex.

Fig. 10 Pressure - Displacement curve of Case 1 scenario

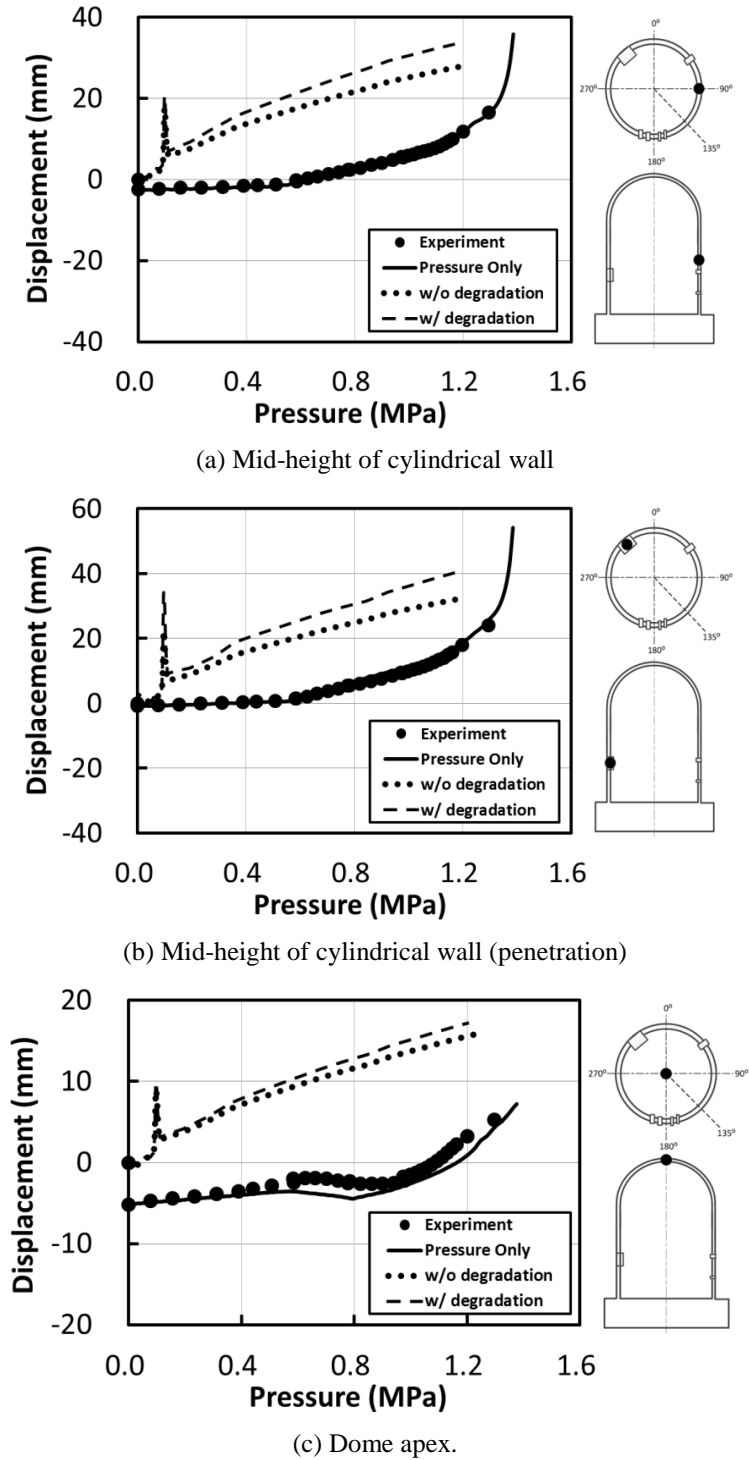


Fig. 11 Pressure - Displacement curve of Case 2 scenario

#### 4. Conclusions

In this paper, three-dimensional non-linear analyses considering internal pressure and temperature loadings were conducted to evaluate the severe accident in NPP containments. To take into account the tension stiffening and the bond-slip effects developed at the interface of two adjacent materials of concrete and tendon, a modified stress-strain relation of tendon has been proposed on the basis of the constitutive materials of concrete and steel, and as such they can effectively be used in modeling a large three-dimensional PSC structures. The finite element modeling of PCCV has been verified through a comparison of experimental results and numerical results for the 1/4 PCCV which was tested under internal pressure loading condition. From the numerical analyses considering the additional nonlinear effect induced from the elevated temperature, furthermore, the following conclusions were obtained: (1) due to the degradation of mechanical properties of which elastic modulus and strength, its ultimate strength have been down up to 15%; (2) in addition to temperature effect to PCCV, the duration of high temperature also affects to the non-linear behavior of structure as one of major influencing factors; and (3) comparing the analysis results, the structural behavior can be largely affected by high temperature and its duration. Therefore, ignorance of the temperature effect may cause about 10 to 20% overestimation to the ultimate capacity of PCCV. It means that the temperature loading as well as the change in the material properties with temperature must be taken into consideration to exactly predict the nonlinear behavior of PCCV up to reach the ultimate loading condition.

#### Acknowledgments

This work was supported by the Innovations in Nuclear Power Technology of the Korea Institute of Energy Technology Evaluation and Planning (20101620100050) grant funded by the Korea government Ministry of Knowledge Economy. And also, this research was supported by a grant from a Construction Technology Research Project (Development of impact/blast resistant HPRCC and evaluation technique thereof) funded by the Ministry on Land, Infrastructure, and Transport.

#### References

- Anderberg, Y. (1988), "Modelling steel behavior", *Fire Saf. J.*, **13**(1), 17-26.
- Anderberg, Y. and Thelandersson, S. (1976), *Stress and Deformation Characteristics of Concrete at High Temperatures. 2. Experimental Investigation and Material Behavior Model*, Bulletin of Division of Structural Mechanics and Concrete Construction, Bulletin 54.
- Bazant, Z.P. and Kaplan, M.F. (1996), *Concrete at High Temperature, Material Properties and Mathematical Models*, Longman Group Limited, Essex, England.
- Comite Euro-International du Beton (CEB) and Federation International de la Prestressing (FIP) (1990), *CEB-FIP Model Code for Concrete Structures*, Thomas Telford.
- Cruz, C.R. (1968), *Apparatus for Measuring Creep of Concrete at High Temperatures*, Portland Cement Association, Skokie, Illinois, Report, No. 225, 36-42.
- Dameron, R.A., Hansen, B.E., Parker, D.R., Rashid, Y.R., Hessheimer, M. and Costello, J.F. (2003), *Posttest Analysis of the NUPEC/NRC 1:4 Scale Prestressed Concrete Containment Vessel Model*, NUREG/CR-6809, SAND2003-0839P, ANA-01-0330. San Diego, CA, ANATECH Corporation,

- Albuquerque, NM, Sandia National Laboratories.
- Dassault Systemes Simulia Corp. (2010), *Abaqus User's Manual, Version 6.10*, Rhode Island, USA.
- Davie, C.T., Pearce, C.J. and Bićanić, N. (2014), "Fully coupled, hygro-thermo-mechanical sensitivity analysis of a pre-stressed concrete pressure vessel", *Eng. Struct.*, **59**, 536-551.
- Dong, Q., Li, Q.M. and Zheng, J.Y. (2010), "Further study on strain growth in spherical containment vessels subjected to internal blast loading", *Int. J. Impact Eng.*, **37**(2), 196-206.
- Donten, K., Knauff, M., Sadowski, A. and Scibak, W. (1980), "Tests on a model of prestressed reactor containment", *Arch. Civ. Mech. Eng.*, **26**(1), 231-245.
- Eurocode 2 (2004), *Design of Concrete Structures. Part 1-2: General Rules-Structural Fire Design, EN 1992-1-2*, Commission of European Communities, Brussels.
- Harmathy, T.Z. (1993), *Fire safety design and concrete*, Longman Scientific and Technical, Harlow.
- Hessheimer, M.F. and Dameron, R.A. (2006), *Containment Integrity Research at Sandia National Laboratories*, Division of Fuel, Engineering and Radiological Research, Office of Nuclear Regulatory Research, US Nuclear Regulatory Commission.
- Hessheimer, M.F., Shibata, S. and Costello, J.F. (2002), *Results of Overpressurization Test of a 1: 4-Scale Prestressed Concrete Containment Vessel Model*, The ASME Foundation, Inc., Three Park Avenue, New York, NY 10016-5990 (United States).
- Hu, H.T. and Lin, Y.H. (2006), "Ultimate analysis of PWR prestressed concrete containment subjected to internal pressure", *Int. J. Pres. Ves. Pip.*, **83**(3), 161-167.
- Kevrokian, S., Heinfling, G. and Courtois, A. (2005), "Prediction of containment vessel mock up cracking during over design pressure test", *Proceedings of Transactions of the 18th International Conference on Structural Mechanics in Reactor Technology (SMiRT 18)*, Beijing, China.
- Kodur, V., Dwaikat, M. and Fike, R. (2010), "High-temperature properties of steel for fire resistance modeling of structures", *J. Mater. Civil Eng.*, **22**(5), 423-434.
- Kupfer, H.B. and Gerstle, K.H. (1973), "Behavior of concrete under biaxial stresses", *J. Eng. Mech. ASCE*, **99**(4), 853-866.
- Kwak, H.G. and Kim, D.Y. (2004a), "Material nonlinear analysis of RC shear walls subject to monotonic loadings", *Eng. Struct.*, **26**(11), 1517-1533.
- Kwak, H.G. and Kim, D.Y. (2004b), "Material nonlinear analysis of RC shear walls subject to cyclic loadings", *Eng. Struct.*, **26**(10), 1423-1436.
- Kwak, H.G. and Kim, D.Y. (2006a), "Cracking behavior of RC panels subject to biaxial tensile stresses", *Comput. Struct.*, **84**(5), 305-317.
- Kwak, H.G. and Kim, J.H. (2006b), "Numerical models for prestressing tendons in containment structures", *Nucl. Eng. Des.*, **236**(10), 1061-1080.
- Lee, H.P. (2011), "Shell finite element of reinforced concrete for internal pressure analysis of nuclear containment building", *Nucl. Eng. Des.*, **241**(2), 515-525.
- Lee, J. and Fenves, G.L. (1998), "Plastic-damage model for cyclic loading of concrete structures", *J. Eng. Mech. ASCE*, **124**(8), 892-900.
- Lie, T.T. and Chabot, M. (1990), "A method to predict the fire resistance of circular concrete filled hollow steel columns", *J. Fire Prot. Eng.*, **2**(4), 111-124.
- Lie, T.T. and Lin, T.D. (1985), "Fire performance of reinforced concrete columns", *ASTM STP*, **882**, 176-205.
- McGregor, J.G., Simmonds, S.H. and Rizkalla, S.H. (1980), "Test of a prestressed secondary containment structure", Struct. Eng. Rep. Department of Civil Engineering, University of Alberta, Edmonton, Canada.
- Mathet, E., Hessheimer, M.F., Ali, S. and Tegeler, B. (2005), "An international standard problem: analysis of 1: 4-scale prestressed concrete containment vessel model under severe accident conditions", *Proceedings of 18th International Conference on Structural Mechanics in Reactor Technology, SMiRT (Vol. 18)*, Beijing, China.
- Nahas, G. and Cirée, B. (2007), "Mechanical analysis of the containment building behavior for the French, PWR 900 MWe under severe accident", *Proceedings of 19th International Conference on Structural Mechanics in Reactor Technology. SMiRT (Vol. 19)*, Toronto, USA.

- Noh, S.H., Moon, I.H., Lee, J.B. and Kim, J.H. (2008), "Analysis of Prestressed Concrete Containment Vessel (PCCV) under severe accident loading", *Nucl. Eng. Technol.*, **40**(1), 77.
- Parmar, R.M., Singh, T., Thangamani, I., Trivedi, N. and Singh, R.K. (2013), "Over-pressure test on BARCOM pre-stressed concrete containment", *Nucl. Eng. Des.*, **269**(1), 177-183.
- Phan, L.T. and Carino, N.J. (1998), "Review of mechanical properties of HSC at elevated temperature", *J. Mater. Civil Eng.*, **10**(1), 58-65.
- Rizkalla, S.H., Simmonds, S.H. and MacGregor, J.G. (1984), "Prestressed concrete containment model", *J. Struct. Eng. ASCE*, **110**(4), 730-743.
- Schaffer, E.L. (1992), *Structural Fire Protection*, ASCE.
- Schneider, U. (1988), "Concrete at high temperatures-a general review", *Fire Saf. J.*, **13**(1), 55-68.
- Twidale, D. and Crowder, R. (1991), "Sizewell 'B'-a one tenth scale containment model test for the UK PWR programme", *Nucl. Eng. Des.*, **125**(1), 85-93.
- Yonezawa, K., Imoto, K., Watanabe, Y. and Akimoto, M. (2002), "Ultimate capacity analysis of 1/4 PCCV model subjected to internal pressure", *Nucl. Eng. Des.*, **212**(1), 357-379.